S-ROCK METHODS FOR STIFF ITÔ SDEs[*]

ASSYR ABDULLE[†] AND TIEJUN LI[‡]

Abstract. In this paper, we present a class of explicit numerical methods for stiff Itô stochastic differential equations (SDEs). These methods are as simple to program and to use as the well-known Euler-Maruyama method, but much more efficient for stiff SDEs. For such problems, it is well known that standard explicit methods face step-size reduction. While semi-implicit methods can avoid these problems at the cost of solving (possibly large) nonlinear systems, we show that the step-size reduction phenomena can be reduced significantly for explicit methods by using stabilization techniques. Stabilized explicit numerical methods called S-ROCK (for stochastic orthogonal Runge-Kutta Chebyshev) have been introduced in [C. R. Acad. Sci. Paris, 345(10), 2007] as an alternative to (semi-) implicit methods for the solution of stiff stochastic systems. In this paper we discuss a genuine Itô version of the S-ROCK methods which avoid the use of transformation formulas from Stratonovich to Itô calculus. This is important for many applications. We present two families of methods for one-dimensional and multi-dimensional Wiener processes. We show that for stiff problems, significant improvement over classical explicit methods can be obtained. Convergence and stability properties of the methods are discussed and numerical examples as well as applications to the simulation of stiff chemical Langevin equations are presented.

Key words. Stiff stochastic differential equations; Multiscale Systems; Explicit stochastic methods; Runge-Kutta Chebyshev methods; Stiff chemical Langevin equation

AMS subject classifications. 60H35,65C30, 65C20,65L20

1. Introduction

For the numerical solution of many biological, chemical, physical and economical systems modeled by differential equations, the use of explicit methods is often expensive because of time step reduction due to stability issues. Such systems are called stiff. Stiffness is concerned with (local) properties of a differential equation which can affect the stability of a numerical method [10, 14]. The stability concept under consideration in this paper is mean-square stability. Stiff stochastic systems are usually solved numerically by (semi-)implicit methods, since classical explicit methods, for example the well-known Euler-Maruyama method, face severe time step reduction. This comes at the cost of solving linear algebra systems at each step. It can be expensive for large systems and complicated to implement for complex problems. Furthermore, one faces issues with the convergence of numerical methods for nonlinear systems. Of course for many problems, stiff solvers can be efficient. We show in this paper that whenever implicit computations are to be avoided, one can handle stiff problems much more efficiently than with the classical explicit methods proposed so far in the literature.

We propose a new family of explicit methods for stiff Itô stochastic differential equations (SDEs) with extended stability properties based on the recently developed S-ROCK methods for Stratonovich SDEs [4, 3]. We consider a stiff system of SDEs

$$dY = f(t,Y)dt + \sum_{l=1}^{M} g_l(t,Y)dW_l(t), \quad Y(0) = Y_0, \tag{1.1}$$

[†]School of Mathematics and Maxwell Institute for Mathematical Sciences, University of Edinburgh, Edinburgh EH9 3JZ, UK, (a.abdulle@ed.ac.uk).
[‡]LMAM and School of Mathematical Sciences, Peking University, Beijing 100871, P.R. China, (tieli@pku.edu.cn).

where $Y(t)$ is a random variable with value in $\mathbb{R}^d$, $f:[0,T]\times\mathbb{R}^d\rightarrow\mathbb{R}^d$ is the drift term, $g:[0,T]\times\mathbb{R}^d\rightarrow\mathbb{R}^d$ is the diffusion term and $W_l(t)$ are independent Wiener processes. We will assume usual conditions on f and g (continuity, uniform Lipschitz continuity with respect to the second variable and a linear growth condition) and on Y_0 (independence of the Wiener processes and finite second order moment) to ensure existence and uniqueness of a (mean square bounded) strong solution of (1.1) (see for example [20, Chapter 5.2] for details). For the numerical solution of (1.1), we consider one-step linear methods of the form

$$Y_{n+1} = \Phi(Y_n, h, I_{n_1}, \ldots, I_{n_M}), \qquad (1.2)$$

where $I_{n_l} = W_l(t_{n+1}) - W_l(t_n)$ are independent Wiener increments drawn from the normal distributions with zero mean and variance $h = t_{n+1} - t_n$. In this paper, we are interested in mean-square stable stiff SDEs. We notice, as observed in [16], that stiff solvers can perform poorly for fast/slow stochastic systems with nontrivial invariant measure for the fast system. These problems are not mean-square stable and other approaches are needed for their numerical solution as, for example, the multiscale methods developed in [25] and [7].

Clearly any Itô stochastic differential equation can be converted into Stratonovich form. Thus, the numerical methods proposed in [4] apply to general SDEs. This conversion, however, requires to differentiate the diffusion terms, which can be cumbersome. For many problems modeled by Itô SDEs, for example chemical reactions, dynamical systems used in finance, or stochastic partial differential equations (SPDEs) discretized by the method of lines, it is preferable to have a scheme available directly in the Itô form. It is thus of interest to develop the S-ROCK methods directly for the Itô calculus. We emphasize that the Itô S-ROCK methods are not a straightforward adaptation of the Stratonovich S-ROCK methods [4, 3] and new family of schemes need to be derived and analyzed.

This paper is organized as follows. In section 2 we recall the needed convergence and stability concepts. We then discuss briefly the (deterministic) Chebyshev methods in section 3. In section 4 we introduce the Itô S-ROCK methods, and study their convergence and stability properties. Finally, we present a numerical study of the new methods and applications to the simulation of stiff chemical Langevin equations to illustrate their performance.

2. Classical methods for SDEs

In this section we recall briefly basic concepts about numerical methods for SDEs, important for the derivation of our new methods.

2.1. Convergence. A method is said to have a strong order ρ, respectively weak order of ρ, if there exists a constant C such that

$$\mathbb{E}(|Y_N - Y(\tau)|) \leq Ch^\rho, \quad \left|\mathbb{E}(G(Y_N)) - \mathbb{E}(G(Y(\tau)))\right| \leq Ch^\rho \qquad (2.1)$$

for any fixed $\tau = Nh \in [0,T]$, with h sufficiently small and for all functions $G:\mathbb{R}^d\rightarrow\mathbb{R}$, that are $2\rho+1$ times continuously differentiable with partial derivatives with polynomial growth.

The following two fundamental theorems derived by Milstein set the relation between local and global order of convergence.

THEOREM 2.1. *[19, Chapter 1.1] Suppose that f and g, the drift and diffusion of the SDEs (1.1), are continuous on $[0,T]\times\mathbb{R}^d$, sufficiently smooth, and satisfy a uniform*

Lipschitz condition

$$|f(t,y) - f(t,z)| + |g(t,y) - g(t,z)| \leq L|y - z|, \quad \forall t \in [0,T], \ y,z \in \mathbb{R}^d. \qquad (2.2)$$

Suppose further that the one-step method (1.2) satisfies the following strong and mean local order conditions

$$\mathbb{E}(|Y_1 - Y(h)|) \leq Ch^{\rho+1/2}, \qquad (2.3)$$

$$|\mathbb{E}(Y_1) - \mathbb{E}(Y(h))| \leq Ch^{\rho+1}. \qquad (2.4)$$

Then the method converges with a strong global order ρ.

We note that this theorem has also been discussed in [6] in the framework of tree theory and B-series, originally developed for ODEs [10] .

THEOREM 2.2. *[19, Chapter 2.2] Suppose that f and g, the drift and diffusion of the SDEs (1.1), are continuous on $[0,T] \times \mathbb{R}^d$, satisfy the uniform Lipschitz condition (2.2), and have uniformly bounded moments $\mathbb{E}(\|Y_n\|^{2r})$, $1 \leq n \leq N$ with respect to N for suficiently large r. Suppose further that f and g have partial derivatives with respect to y of order $2(\rho+1)$ with a polynomial growth and that for all functions $G: \mathbb{R}^d \to \mathbb{R}$, that are $2\rho+1$ times continuously differentiable with partial derivatives with polynomial growth we have*

$$|\mathbb{E}(G(Y_1)) - \mathbb{E}(G(Y(h)))| \leq C(Y_0)h^{\rho+1}, \qquad (2.5)$$

where $C(y)$ has a polynomial growth. Then the method converges with a weak global order ρ.

2.2. Stability.   Stability analysis for numerical methods is motivated by the question of the choice of the stepsize h for (1.2) in order to reproduce the characteristic dynamics of the true solution. In order to investigate such a question for numerical schemes, we consider a linear test problem with multiplicative noise [23]

$$dY = \lambda Y \, dt + \mu Y \, dW(t), \quad Y(0) = Y_0, \qquad (2.6)$$

where $\lambda, \mu \in \mathbb{C}$. The solution of (2.6), $Y(t) = Y_0 \exp((\lambda - \frac{1}{2}\mu^2)t + \mu W(t))$, is mean-square stable if and only if

$$\lim_{t \to \infty} \mathbb{E}(|Y(t)|^2) = 0 \iff (\lambda, \mu) \in \mathcal{S}_{\text{SDE}} := \{(\lambda, \mu) \in \mathbb{C}^2; \text{Re}(\lambda) + \frac{1}{2}|\mu|^2 < 0\}, \qquad (2.7)$$

where the right-hand side of (2.7) will be referred as the stability domain of the test equation (2.6). This test problem gives insight of the behavior of (1.1) by linearization around fixed points. Applying the numerical scheme (1.2) to the test problem (2.6), squaring the result, and taking the expectation, we obtain

$$\mathbb{E}(|Y_{n+1}|^2) = R(p,q)\mathbb{E}(|Y_n|^2), \qquad (2.8)$$

where $p = h\lambda, q = \sqrt{h}\mu$ and where $R(p,q)$ is a polynomial in $\text{Re}(p)$, $\text{Im}(p)$, $\text{Re}(q)$, $\text{Im}(q)$. The numerical method is mean-square stable for this test problem if and only if

$$\lim_{n \to \infty} \mathbb{E}(|Y_n|^2) = 0 \iff (h\lambda, \sqrt{h}\mu) \in \mathcal{S} := \{p,q \in \mathbb{C}; R(p,q) < 1\}. \qquad (2.9)$$

Examples. A well-known method for the solution of (1.1) is the Euler-Maruyama scheme, given by

$$Y_{n+1} = Y_n + hf(t, Y_n) + \sum_{l=1}^{M} I_{n_l} g_l(t, Y_n), \qquad (2.10)$$

where $I_{n_l} = W_l(t_{n+1}) - W_l(t_n)$ are independent Wiener increments. This method has strong order $1/2$ and weak order 1 [14]. Applied to the test problem (2.7), we obtain

$$R(p, q) = |1 + p|^2 + q^2 \qquad (2.11)$$

and thus it is mean-square stable if and only if

$$(h\lambda, \sqrt{h}\mu) \in \mathcal{S}_{\mathrm{EM}} := \{p, q \in \mathbb{C}; |1 + p|^2 + q^2 < 1\}.$$

The domain $\mathcal{S}_{\mathrm{EM}}$ is plotted in Figure 2.1 in the $(p, q) = (h\lambda, \sqrt{h}\mu)$ plane (for $\lambda, \mu \in \mathbb{R}$). The left part of the parabola with a boundary given by a dotted curve represents the stability region of the test equation (2.6). We observe that for $|\lambda|, |\mu| \gg 1$ (stiffness), severe stepsize reduction occurs for these methods to be stable. For SDEs with a one-dimensional Wiener process, higher (strong) order methods can be obtained as, for example the Platen method [14] which has strong order 1 and is given by

$$K_n = Y_n + hf(t, Y_n) + \sqrt{h}g(t, Y_n)$$
$$Y_{n+1} = Y_n + hf(t, Y_n) + I_n g(t, Y_n) + \frac{1}{2\sqrt{h}}(g(K_n) - g(Y_n))(I_n^2 - h). \qquad (2.12)$$

We note that higher weak order methods in the framework of the Runge-Kutta methods have been studied in [22].

Applying the method (2.12) to the test problem (2.7) we obtain its stability domain S_{PL} similarly as explained above for the Euler-Maruyama method. We see again in Figure 2.1 that the stability region covers only a small part of the stability region of the test equation.
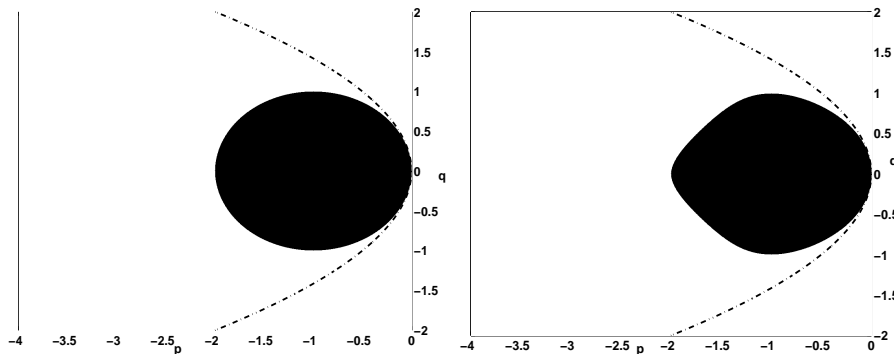

FIG. 2.1. *Mean-square stability domains for the Euler-Maruyama method (left figure) and the Platen method (right figure).*

REMARK 2.3. We notice that some other authors use the representation $(p, q) = (h\lambda, h\mu^2)$ for plotting stability domains. With this scaling, the stability region for

the test problem becomes a wedge. For the class of methods we are constructing this scaling has some drawback: the stability domains of our new methods increase *quadratically* along the p axis (see Figure 4.1) and this remarkable property is somehow hidden (in the plots) with stability domains scaled as $(p,q) = (h\lambda, h\mu^2)$ instead of $(p,q) = (h\lambda, \sqrt{h}\mu)$.

To describe more precisely the mean square stability region of a numerical method, we define a "portion" of the stability domain (2.7) by

$$\mathcal{S}_{\text{SDE},r} = \{(p,q) \in [-r,0] \times \mathbb{R}; |q| \leq \sqrt{-p}\}, \tag{2.13}$$

where $r > 0$. We then consider two parameters l and d related to a numerical stability domain $\mathcal{S}$ by

$$l = \max\{|p|; p < 0, \ [p,0] \subset \mathcal{S}\}, \quad d = \max\{r > 0; \mathcal{S}_{\text{SDE},r} \subset \mathcal{S}\}. \tag{2.14}$$

Clearly, $d \leq l$. We notice that l is a parameter of the stability which corresponds to the noise-free behavior. For SDEs, the parameter d is thus the relevant quantity to optimize. For the Euler-Maruyama and the Platen methods we have $l_{\text{EM}} = 2, l_{\text{PL}} = 2, d_{\text{EM}} \simeq 1/4, d_{\text{PL}} \simeq 1/4$. The goal is to construct a family of numerical methods with d much larger than the above values, typical for any "traditional" explicit methods.

3. Chebyshev and ROCK methods

The stochastic methods proposed in this paper are special families of (1.2) based on Chebyshev methods. In this section we briefly review Chebyshev methods, originally proposed for stiff ordinary differential equations.

Chebyshev methods. The idea behind our stochastic methods is to extend a class of stabilized numerical methods introduced by Saul'ev, Franklin and Guillou & Lago (see [10, Section IV.2] and the references therein) for the numerical solution of ODEs

$$Y' = f(t,Y), \quad Y(0) = Y_0$$

with a Jacobian matrix having negative eigenvalues with large magnitude. Such methods, further developed in [1, 2, 15, 24] have proved to be very efficient for large stiff systems of deterministic differential equations. They rely on stability functions given by shifted Chebyshev-like polynomials $R_m(z) = T_m(1 + z/m^2)$, where $T_m(z)$ is the Chebyshev polynomial of degree m. The polynomials $R_m(z)$ equi-oscillate between -1 and 1 and have the property that $|R_m(z)| \leq 1$ for $z \in [0, 2m^2]$. The related stability domains are therefore extended along the negative real axis and they increase *quadratically* with the degree m of $R_m(z)$. The degree m of the stability functions indicates the stage number of the associated Runge-Kutta method, while the property $R_m(z) = 1 + z + \mathcal{O}(z^2)$ ensures the first order convergence of the numerical method. These methods have been originally developed for problems with eigenvalues along the negative real axis. A typical stability domain $\mathcal{S}_m$ is sketched in Figure 3.1, where

$$\mathcal{S}_m := \{z \in \mathbb{C}; |R_m(z)| < 1\}.$$

It can be seen in Figure 3.1 that the boundary of the stability domain along the negative real axis is 200, for $m = 10$. However, there are regions in $[0,200]$, precisely when $T(1 + z/m^2) = 1$, with no stability on the imaginary axis.

To overcome the aforementioned issue, it has been suggested by Guillou and Lago to replace the requirement $|R_m(z)| \leq 1$ by $|R_m(z)| \leq \eta < 1$. This can be achieved
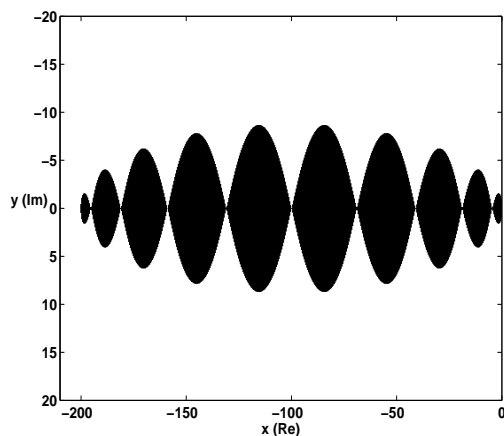
FIG. 3.1. *Stability domain of first order Chebyshev method (degree $m = 10$).*

for the polynomials $T_m(1 + z/m^2)$ by dividing it by the quantity $T_m(\omega_0) > 1$, where $\omega_0 = 1 + \eta/m^2$. To obtain the correct order with this modified stability function, one does a change of variables and obtains $R_{m,\eta}(z) = \frac{T_m(\omega_0 + \omega_1 z)}{T_m(\omega_0)}$, where $\omega_1 = \frac{T_m(\omega_0)}{T'_m(\omega_0)}$ (see [10, Section IV.2]). By increasing the paramter η the strip around the negative real axis included in the stability domain can be enlarged as can be seen in Figure 3.1.
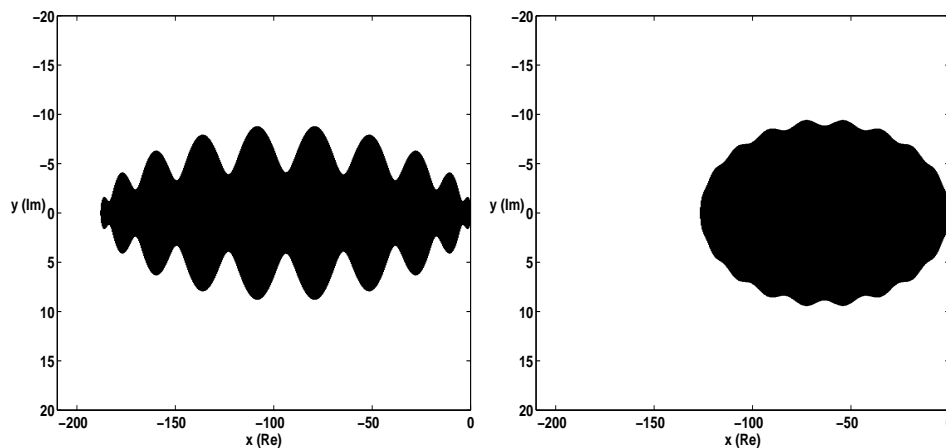

FIG. 3.2. *Stability domain of first order Chebyshev methods (degree $m = 10$) with variable damping $\eta = 0.1$ (left figure), $\eta = 1$ (right figure).*

Higher order quasi-optimal Chebyshev methods: the ROCK methods.
Higher order methods, called ROCK, for orthogonal Runge-Kutta Chebyshev methods, based on orthogonal polynomials have been developed in [1, 2]. The stability functions are given by polynomials $R_m(z) = 1 + z + \ldots + z^p/p! + \mathcal{O}(z^{p+1})$ of order p and degree m with quasi-optimal stability domains along the negative real axis. These

polynomials can be decomposed as

$$R_m(z) = w_p(z)P_{m-p}(z),$$

where $P_{m-p}(z)$ is a member of a family of polynomials $\{P_j(z)\}_{j\geq 0}$ which are orthogonal with respect to the weight function $\frac{w_p(z)^2}{\sqrt{1-z^2}}$. The idea for the construction of a numerical method is then as follows: the 3-term recurrence relation of the orthogonal polynomials $\{P_j(z)\}_{j\geq 0}$

$$P_j(z) = (\alpha_j z - \beta_j)P_{j-1}(z) - \gamma_j P_{j-2}(z),$$

is used to define the internal stages of the method

$$K_j = h\alpha_j f(K_{j-1}) - \beta_j K_{j-1} - \gamma_j K_{j-2}, \; j=2,\ldots,m-p.$$

This ensures the good stability properties of the method. A p-stage finishing procedure with the polynomial $w_p(z)$ as underlying stability function, ensures the right order of the method.

4. The Itô S-ROCK methods

In this section we construct and analyze the Itô S-ROCK methods. Inspired by the above ROCK methods and the Stratonovich S-ROCK methods developed in [4], we consider methods based on

- deterministic Chebyshev-like internal stages to ensure good stability properties,
- a finishing stochastic procedure to incorporate the diffusion part and obtain the desired stochastic convergence properties.

As for deterministic methods, the use of damping plays a crucial role and allows to enlarge the width of the stability domains.

4.1. Weak order 1, strong order 1/2 Itô S-ROCK methods.

We consider a family of stochastic methods for general multi-dimensional stiff Itô SDEs. We define a m-stage method by

$$
\begin{aligned}
K_0 &= Y_n, \\
K_1 &= Y_n + h\frac{\omega_1}{\omega_0}f(K_0), \\
K_j &= 2h\omega_1\frac{T_{j-1}(\omega_0)}{T_j(\omega_0)}f(K_{j-1}) + 2\omega_0\frac{T_{j-1}(\omega_0)}{T_j(\omega_0)}K_{j-1} - \frac{T_{j-2}(\omega_0)}{T_j(\omega_0)}K_{j-2}, \\
&\quad j=2,\ldots,m-1, \\
K_m &= 2h\omega_1\frac{T_{m-1}(\omega_0)}{T_m(\omega_0)}f(K_{m-1}) + 2\omega_0\frac{T_{m-1}(\omega_0)}{T_m(\omega_0)}K_{m-1} - \frac{T_{m-2}(\omega_0)}{T_m(\omega_0)}K_{m-2} \\
&\quad + \sum_{l=1}^{M} I_{n_l}g_l(K_{m-1}),
\end{aligned}
\tag{4.1}
$$

where $\omega_0 = 1 + \frac{\eta}{m^2}$, $\omega_1 = \frac{T_m(\omega_0)}{T_m'(\omega_0)}$. The approximation at step $n+1$ is then defined by $Y_{n+1} := K_m$. The following two theorems give the convergence properties of the methods (4.1).

THEOREM 4.1. *For $m \geq 2$, the methods (4.1) have strong global order 1/2.*
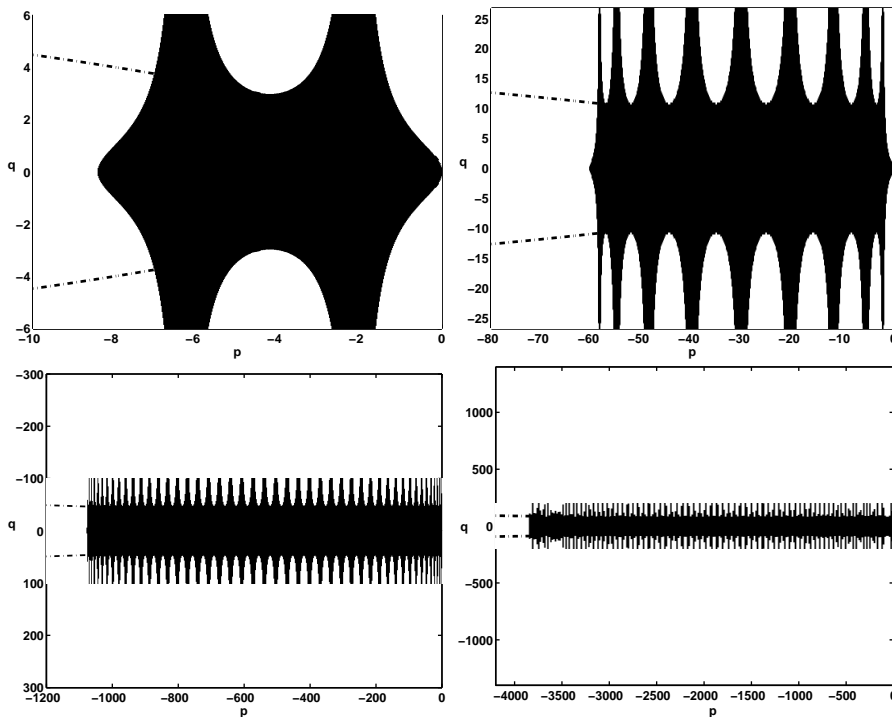
FIG. 4.1. *Stability domains of Itô S-ROCK methods (4.1) for $m=3$ (upper left picture), $m=10$ (upper right picture), $m=50$ (lower left picture) and $m=100$ (lower right picture).*

Proof. The proof is obtained by expanding (4.1) in Taylor series and estimating the local truncation errors. We first obtain for the deterministic stages $(1 \leq j \leq m-1)$

$$K_j = Y_n + h\omega_1 \frac{T'_j(\omega_0)}{T_j(\omega_0)} f(Y_n) + \mathcal{O}(h^2), \tag{4.2}$$

using the recurrence relation of the Chebyshev polynomials. For the last stage we have

$$K_m = Y_n + h\omega_1 \frac{T'_m(\omega_0)}{T_m(\omega_0)} f(Y_n) + \sum_{l=1}^{M} I_{n_l} \left(g_l(Y_n) + h\omega_1 \frac{T'_{m-1}(\omega_0)}{T_{m-1}(\omega_0)} g'_l(Y_n) f(Y_n) \right)$$
$$+ \mathcal{O}(I_{n_l} h^2) + \mathcal{O}(h^2)$$
$$= Y_n + h f(Y_n) + \sum_{l=1}^{M} I_{n_l} g_l(Y_n) + \mathcal{O}(I_{n_l} h), \tag{4.3}$$

where $g'_l(Y_n)$ represent a Jacobian matrix and where we used that $\omega_1 \frac{T'_m(\omega_0)}{T_m(\omega_0)} = 1$.

We compare now the expression for $K_m = Y_{n+1}$ with the Itô Taylor-Platen expansion of the exact solution of (1.1) after one step with initial condition $Y(t_n) = Y_n$

$$Y(t_{n+1}) = Y_n + h f(Y_n) + \sum_{l=1}^{M} g_l(Y_n) \int_{t_n}^{t_{n+1}} dW_l + R_e, \tag{4.4}$$
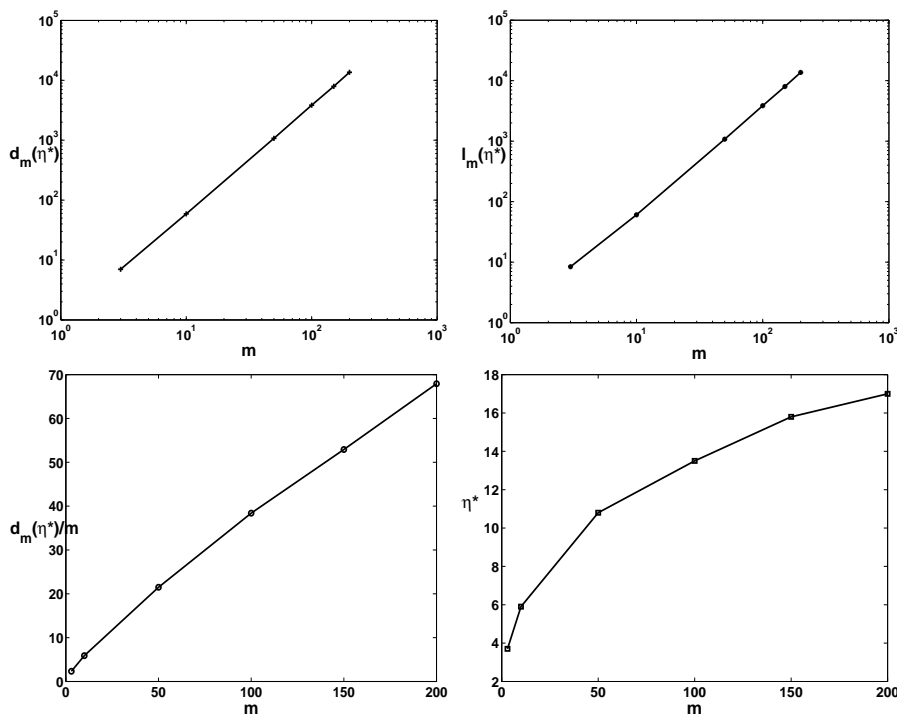
FIG. 4.2. *The above four figures show the stability domains study for the Itô S-ROCK methods (4.1). They are shown as optimal values $d_m^{\eta^*}$ for $3 \leq m \leq 200$ defined in (4.11) (upper left plot), and corresponding l^{η^*} defined in (2.14) (upper right plot), the ratio $d_m^{\eta^*}/m$ representing the stability versus work (lower left plot) and optimal values of η for $m \leq 200$ (lower right plot).*

where $\mathbb{E}|R_e| = \mathcal{O}(h)$ and $|\mathbb{E}(R_e)| = \mathcal{O}(h^2)$.

Defining $Y(t_{n+1}) - Y_{n+1} = e$, a simple calculation shows that

$$\mathbb{E}|e| = \mathcal{O}(h) \text{ and } |\mathbb{E}(e)| = \mathcal{O}(h^2).$$

Using Theorem 2.1 completes the proof.   □

We next study the weak order of the S-ROCK methods.

THEOREM 4.2. *For $m \geq 2$, the methods (4.1) have weak global order 1.*

Proof. Let Y_1 be the approximation of a given S-ROCK method (4.1) and $Y(h)$ be the exact solution at time h. Comparing (4.3) and (4.4) (for $n=0$) and using Taylor expansion, assuming suitable smoothness of the function G (see 2.1), gives

$$|\mathbb{E}(f(Y_1)) - \mathbb{E}(f(Y(h)))| \leq C(Y_0)h^2,$$

where the lower order terms either vanish because they cancel each other or become zero after taking the expectation (any expression containing an even number of Wiener increments vanishes after taking the expectation).

To conclude the proof, one needs the uniform bound of $\mathbb{E}\|Y_n\|^{2r}$ for any $r \in \mathbb{N}$.

Here we follow the lines in [19] (Lemma 2.2, pp. 102). What we need is

$$|\mathbb{E}(Y_{n+1}-Y_n|Y_n)| \leq C_1(1+|Y_n|)h, \tag{4.5}$$

$$|Y_{n+1}-Y_n| \leq M(\xi_n)(1+|Y_n|)h^{\frac{1}{2}} \tag{4.6}$$

for a positive constant C_1. Here ξ_n denotes random variables related to the Wiener increments I_n and $M(\xi_n)$ must have moments of all orders, i.e., $\mathbb{E}(M(\xi_n))^i \leq C_2$ for $i \in \mathbb{N}$. To prove (4.5), we only need to consider the scheme (4.1) without the diffusion terms, which vanish after taking the expectation. A straightforward mathematical induction implies the following bounds

$$|K_j - Y_n| \leq C_j h(1+|Y_n|), \ j=0,\ldots,m-1 \tag{4.7}$$

by utilizing the linear growth condition of $f(y)$. The last step in the induction gives (4.5). Note that the only difference between (4.5) and (4.6) for the scheme (4.1) is the diffusion part, so we obtain (4.6) through direct calculation defining $\xi_n = I_n/\sqrt{h}$ and using the linear growth condition of $g(y)$. The above choice for ξ_n ensures that $M(\xi_n)$ has moments of all orders (for a given h_0 and $h \leq h_0$). Finally we complete the proof by applying Theorem 2.2. □

Study of the mean-square stability. We apply the method (4.1) to the linear test problem (2.6) and obtain

$$K_j = \frac{T_j(\omega_0+\omega_1 p)}{T_j(\omega_0)} Y_n \ j=0,1,\ldots,m-1$$

for the internal stages and

$$Y_{n+1} = K_m = \left(\frac{T_m(\omega_0+\omega_1 p)}{T_m(\omega_0)} + V_n q \frac{T_{m-1}(\omega_0+\omega_1 p)}{T_{m-1}(\omega_0)}\right) Y_n, \tag{4.8}$$

after one step, where V_n is a $N(0,1)$ Gaussian random variable and where we used the notation $I_n = \sqrt{h}V_n$ and $q = \sqrt{h}\mu$.

Squaring and taking the expectation gives a mean-square stability function

$$R_m(p,q) = \frac{T_m^2(\omega_0+\omega_1 p)}{T_m^2(\omega_0)} + q^2 \frac{T_{m-1}^2(\omega_0+\omega_1 p)}{T_{m-1}^2(\omega_0)}. \tag{4.9}$$

For a given m (stage number) we denote by $\mathcal{S}_m^\eta$ the stability domain (2.9) of the related method (4.1), where we add an index η since the method depends on the parameter η (damping) through ω_0 and ω_1. $\mathcal{S}_{\text{SDE},d_m(\eta)}$ is then the largest portion of the true stability domain included in $\mathcal{S}_m^\eta$ as defined in (2.13). Notice that d defined in (2.14) depends now on η. The parameter l defined in (2.14) related to the stability region along the p axis will depend on m and η, and we will denote it by $l_m(\eta)$.

The following lemmas characterize the stability domains of our methods. Their proofs can be obtained following the lines of [4].

LEMMA 4.3. *Let $\eta \geq 0$. For all m, the m-stage numerical method (4.1) has a mean square stability region $\mathcal{S}_m^\eta$ with $l_m(\eta) \geq c(\eta)m^2$, where $c(\eta)$ depends only on η.*

LEMMA 4.4.

$$l_m(\eta) \to 2m \ \text{ for } \ \eta \to \infty. \tag{4.10}$$

In view of the above two lemmas we make the following important observation: for any fixed η, the stability domain along the p axis increases quadratically (Lemma 4.3), but for a given method, i.e., a fixed m, increasing the damping to infinity reduces the quadratic growth along the p axis into a linear growth (Lemma 4.4). Since $d_m(\eta) \leq l_m(\eta)$ no gain compared to classical methods can be obtained in this limit case.

Optimized methods. Our goal is now for a given method to find the value of η, denoted η^* which maximize $d_m(\eta)$, i.e.,

$$\eta^* = \operatorname{argmax}\{d_m(\eta); \eta \in [0, \infty)\}. \qquad (4.11)$$

The corresponding optimal values $d_m(\eta^*)$ for $m \leq 200$ have been computed numerically and are reported in Figure 4.2 (upper right plot). We also report in the same figure the values of $l_m(\eta^*)$ (upper left plot) and η^* (lower right plot). We see that for $\eta = \eta^*$, $d_m(\eta^*) \simeq l_m(\eta^*)$. In the third picture of Figure 4.2 (lower left plot) we study the efficiency of the method.

Since a large number of stages is allowed, the Itô S-ROCK methods will be efficient only if the ratio $d_m(\eta^*)/m$ (stability versus work) is larger than the corresponding value for classical methods. We see that this is indeed the case. A comparison with the two "classical" methods discussed in the beginning of the paper, the Euler-Maruyama and the Platen methods, for which $d_{\mathrm{EM}}/m = 1/4, d_{\mathrm{PL}}/m = 1/8$ (with $m = 2$), shows that the S-ROCK methods have a work/stability ratio up to 272, respectively 543 times larger.

4.2. Weak order 1, strong order 1 Itô S-ROCK methods for SDEs with commutativity properties. If $M = 1$ (one-dimensional Wiener process), for diagonal or commutative noise, it is possible to modify the methods (4.1) in order to obtain a strong order 1 Itô S-ROCK methods. In what follows we give the formulas for the case $M = 1$ and will comment on the diagonal and commutative cases.

The higher strong order m-stage S-ROCK methods are defined for $m \geq 3$ as follows

$$
\begin{aligned}
K_0 &= Y_n, \\
K_1 &= Y_n + h\frac{\omega_1}{\omega_0}f(K_0), \\
K_j &= 2h\omega_1\frac{T_{j-1}(\omega_0)}{T_j(\omega_0)}f(K_{j-1}) + 2\omega_0\frac{T_{j-1}(\omega_0)}{T_j(\omega_0)}K_{j-1} - \frac{T_{j-2}(\omega_0)}{T_j(\omega_0)}K_{j-2}, \\
&\quad j = 2, \ldots, m-1, \\
K_{m-1}^* &= K_{m-1} + \sqrt{h}g(K_{m-1}), \\
K_m &= 2h\omega_1\frac{T_{m-1}(\omega_0)}{T_m(\omega_0)}f(K_{m-1}) + 2\omega_0\frac{T_{m-1}(\omega_0)}{T_m(\omega_0)}K_{m-1} - \frac{T_{m-2}(\omega_0)}{T_m(\omega_0)}K_{m-2} \\
&\quad + I_n g(K_{m-1}) + \frac{1}{2\sqrt{h}}(g(K_{m-1}^*) - g(K_{m-1}))(I_n^2 - h). \qquad (4.12)
\end{aligned}
$$

The approximation at the step $n+1$ is then defined by $Y_{n+1} := K_m$.

The case of diagonal noise. We recall that diagonal noise denotes the situation when the dimension d of $Y(t)$ equals M (the number of independent Wiener processes), each component $Y_k(t)$ of the Itô process is only disturbed by the corresponding component W_k of the Wiener process W and $g_k(t, Y)$ depends only on Y_k (see [14, Chapter

10.3] for details). In this case the last term should be understood componentwise,

$$\frac{1}{2\sqrt{h}}(g_k(K^*_{m-1}) - g_k(K_{m-1}))\left(I^2_{n_k} - h\right), \tag{4.13}$$

where g_k represents the k-th component of the vector g and $I_{n_k} = W_k(t_{n+1}) - W_k(t_n)$.

The case of commutative noise. Define the operator

$$L^l = \sum_{k=1}^{d} g_l^k \frac{\partial}{\partial y^k}, \quad l = 1, 2, \ldots, M. \tag{4.14}$$

For abitrary M, if the commutativity condition [14]

$$L^l g_r^k = L^r g_l^k \qquad \forall l, r = 1, \ldots, M; \ k = 1, \ldots, d \tag{4.15}$$

holds for the diffusion functions, then using

$$I_{n_l, n_r} + I_{n_r, n_l} = I_{n_l} I_{n_r} \ (l \neq r) \quad \text{and} \quad I_{n_l, n_l} = \frac{1}{2}(I^2_{n_l} - h), \tag{4.16}$$

where $I_{n_l, n_r} = \int_{t_n}^{t_{n+1}} \int_{t_n}^{\theta} dW_l(\theta_1) dW_r(\theta)$, one replaces two last stages of the methods (4.12) by

$$K^*_{m-1} = K_{m-1} + \sum_{r=1}^{M} g_r(K_{m-1}) I_{n_r},$$

$$K^{**,l}_{m-1} = K_{m-1} + \sqrt{h} g_l(K_{m-1}), \quad l = 1, 2, \ldots, M,$$

$$Y_{n+1} = K_m = 2h\omega_1 \frac{T_{m-1}(\omega_0)}{T_m(\omega_0)} f(K_{m-1}) + 2\omega_0 \frac{T_{m-1}(\omega_0)}{T_m(\omega_0)} K_{m-1} - \frac{T_{m-2}(\omega_0)}{T_m(\omega_0)} K_{m-2}$$

$$+ \sum_{l=1}^{M} I_{n_l} g_l(K_{m-1}) + \frac{1}{2} \sum_{l=1}^{M} (g_l(K^*_{m-1}) - g_l(K_{m-1})) I_{n_l}$$

$$- \frac{1}{2} \sum_{l=1}^{M} \left(g_l(K^{**,l}_{m-1}) - g_l(K_{m-1}) \right) \sqrt{h}. \tag{4.17}$$

Note that we have more intermediate steps here to avoid the computation of the derivatives of functions $g_l(y)$. We next discuss the convergence properties of these methods.

THEOREM 4.5. *If $M = 1$ or for diagonal or commutative noise, the methods (4.12) have strong global order* 1.

Proof. Let us first consider the $M = 1$ case. As for Theorem 4.1, we expand the method (4.12) in Taylor series and estimate the strong and weak local truncation errors. Using (4.2) for the first $m-1$ deterministic stages, expanding K^*_{m-1} and K_m in Taylor series we get

$$K_m = Y_n + h\left(f(Y_n) + \mathcal{O}(h)\right) + I_n\left(g(Y_n) + \mathcal{O}(h)\right)$$

$$+ \frac{1}{2}\left(g'g(Y_n) + \mathcal{O}(h)\right)\left((I_n)^2 - h\right). \tag{4.18}$$

We compare now the expression for $Y_{n+1} = K_m$ with the Itô Taylor-Platen expansion of the exact solution of (1.1) after one step with initial condition $Y(t_n) = Y_n$.

$$Y(t_{n+1}) = Y_n + hf(Y_n) + g(Y_n) \int_{t_n}^{t_{n+1}} dW(\theta)$$

$$+ g'(Y_n)g(Y_n) \int_{t_n}^{t_{n+1}} \int_{t_n}^{\theta} dW(\theta_1)dW(\theta) + R_e, \quad (4.19)$$

where $\mathbb{E}|R_e| = \mathcal{O}(h^{3/2})$ and $|\mathbb{E}(R_e)| = \mathcal{O}(h^2)$. Using the property of the Itô integral,

$$\int_{t_n}^{t_{n+1}} \int_{t_n}^{\theta} dW(\theta_1)dW(\theta) = \frac{1}{2}\left(I_n^2 - h\right).$$

A comparison of the numerical and exact Taylor-Platen series shows that

$$\mathbb{E}|e| = \mathcal{O}(h^{3/2}) \text{ and } |\mathbb{E}(e)| = \mathcal{O}(h^2).$$

Using Theorem 2.1 completes the proof for the one dimensional case. Exactly the same proof can be done for the diagonal noise case. For the commutative case, one observes that a Taylor expansion of the last stage gives

$$Y_{n+1} = Y_n + hf(Y_n) + \sum_{l=1}^{M} I_{n_l}g_l(Y_n) + \frac{1}{2}\sum_{l,r=1}^{M} L^l g_r(Y_n)I_{n_l}I_{n_r} - \frac{1}{2}\sum_{l=1}^{M} L^l g_l h + R_e, \quad (4.20)$$

where $\mathbb{E}|R_e| = \mathcal{O}(h^{3/2})$ and $|\mathbb{E}(R_e)| = \mathcal{O}(h^2)$. Using the commutativity conditions (4.15) and (4.16) we see that the above expression can be written as

$$Y_{n+1} = Y_n + hf(Y_n) + \sum_{l=1}^{M} I_{n_l}g_l(Y_n)$$

$$+ \sum_{l,r=1}^{M} L^l g_r(Y_n) \int_{t_n}^{t_{n+1}} \int_{t_n}^{\theta} dW_l(\theta_1)dW_r(\theta) + R_e. \quad (4.21)$$

A comparison of the numerical and exact Taylor-Platen series shows that

$$\mathbb{E}|e| = \mathcal{O}(h^{3/2}) \text{ and } |\mathbb{E}(e)| = \mathcal{O}(h^2),$$

and we can conclude as for the case $M = 1$ by invoking Theorem 2.1. □

THEOREM 4.6. *For $m \geq 2$, the methods (4.12) have weak global order* 1.

Proof. This can be proved by comparing the expansions (4.18) or (4.20) with the expansion (4.19) of the exact solution, and by following the lines of Theorem 4.2 using the Lipschitz condition and the linear growth conditions of f and g. The details are omitted here. □

REMARK 4.7. In general, the methods (4.12) cannot be of higher weak order since (4.18) shows that already in the deterministic case they do not enjoy second order accuracy.

The study of the mean-square stability can be done in the same manner as for the methods (4.1). We apply the method (4.12) to the linear test problem (2.6) and we obtain

$$Y_{n+1} = \left(\frac{T_m(\omega_0 + \omega_1 p)}{T_m(\omega_0)} + V_n q \frac{T_{m-1}(\omega_0 + \omega_1 p)}{T_{m-1}(\omega_0)} + (V_n^2 - 1) \frac{q^2}{2} \frac{T_{m-1}(\omega_0 + \omega_1 p)}{T_{m-1}(\omega_0)} \right) Y_n,$$
(4.22)

where we used $I_n = \sqrt{h} V_n$ and $q = \sqrt{h}\mu$ as before. Squaring and taking the expectation gives a mean-square stability function

$$R_m(p,q) = \frac{T_m^2(\omega_0 + \omega_1 p)}{T_m^2(\omega_0)} + q^2 \frac{T_{m-1}^2(\omega_0 + \omega_1 p)}{T_{m-1}^2(\omega_0)} + \frac{q^4}{2} \frac{T_{m-1}^2(\omega_0 + \omega_1 p)}{T_{m-1}^2(\omega_0)}.$$
(4.23)

In Figure 4.3 we sketch stability domains for selected stage number m. We note that lemmas 4.3 and 4.4 remain true for the stability domains given by (4.23). As for the
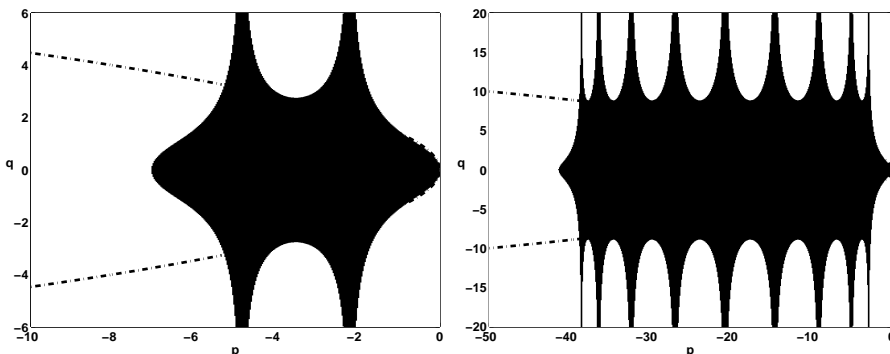

FIG. 4.3. *Stability domains of Itô S-ROCK methods (4.12) for $m = 3$ (left plot) and $m = 10$ (right plot).*

methods (4.1) we compute the optimal values $d_m(\eta^*)$ for $m \le 200$ numerically. These values are reported in Figure 4.4. (upper right plot). We again also report in the same figure the corresponding values of $l_m(\eta^*)$ (upper left plot) and η^* (lower right plot). In the lower left plot of Figure 4.4 we study the efficiency of the method. We wee that the stability domains are shorter than for the methods (4.1) (compare also Figure 4.3 with Figure 4.1). We notice that the values of $d_m(\eta^*)$ are of the same size as the corresponding values obtained for the Stratonovich S-ROCK methods of strong order 1 [3]. We still have a substantial improvement compared to classical explicit methods, since the order 1 Itô S-ROCK methods have a work stability ratio up to 160 and 320 times larger when compared with the Platen and the Euler-Maruyama methods, respectively.

4.3. Error constants. In this section we briefly study the error constant of the S-ROCK methods. Following the theory for deterministic problems, we apply the S-ROCK methods (4.1) or (4.12) to the linear test problem (2.6) (with $Y_0 = 1$) and estimate the constant in front of the leading error terms. As previously, we will use the notation $p = \lambda h, q = \mu\sqrt{h}$. For the exact solution we obtain

$$Y(h) = 1 + p + \frac{1}{2}p^2 + \mathcal{O}(p^3)$$
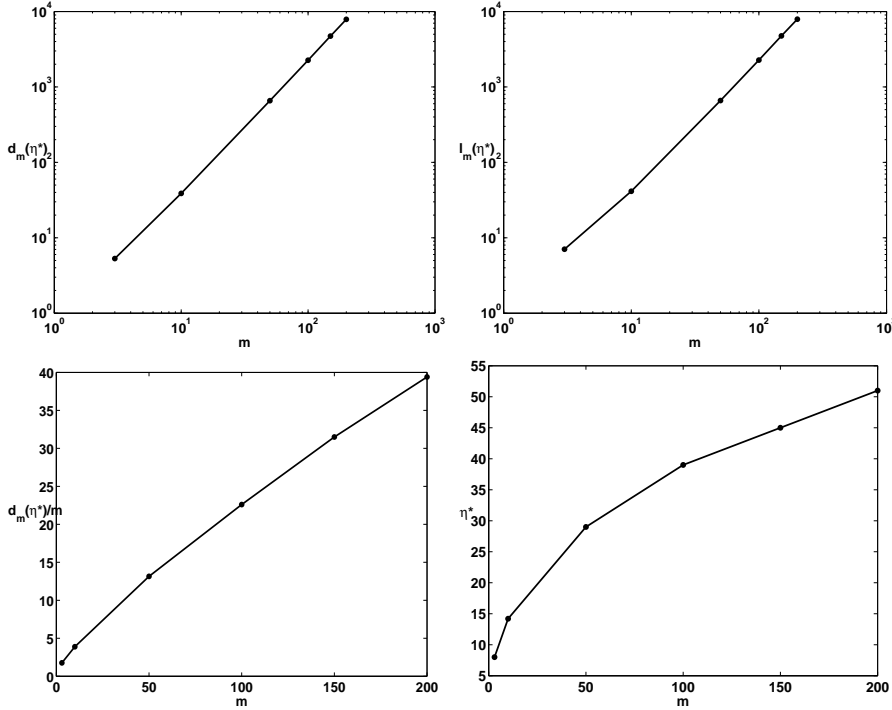$$+ \mu I_1 + \mu^2 I_{11} + \lambda\mu I_0 I_1 + \mu^3 I_{111} + R,$$
(4.24)

FIG. 4.4. *The above four figures show the stability domains study for the Itô S-ROCK methods (4.12). They are shown as optimal values $d_m^{\eta^*}$ for $3 \leq m \leq 200$ defined in (4.11) (upper left plot), and corresponding l^{η^*} defined in (2.14) (upper right plot), the ratio $d_m^{\eta^*}/m$ representing the stability versus work (lower left plot) and optimal values of η for $m \leq 200$ (lower right plot).*

where we used the notation

$$I_{10} = \int_0^h \int_0^\theta dW(\theta_1)d\theta, \; I_{10} = \int_0^h \int_0^\theta d\theta_1 dW(\theta),$$

$$I_{111} = \int_0^h \int_0^\theta \int_0^{\theta_1} dW(\theta_2)dW(\theta_1)dW(\theta).$$

We also used the relation $I_{10} + I_{01} = I_0 I_1$ (see [14] for details). We note that $\mathbb{E}(|R|) = \mathcal{O}(h^2)$ and $\mathbb{E}(R) = 0$.

We observe that the S-ROCK methods applied to the linear test problem (2.6) gives (4.8) and (4.22) for the methods (4.1) and (4.12), respectively. We expand these expressions in Taylor series around ω_0 and further consider the leading terms in the regime $\eta \to \infty$, since we are interested in the parameter range of large damping. We obtain

$$Y_1 = 1 + p + \frac{1}{2}\left(1 - \frac{1}{m}\right)p^2 + \mathcal{O}(p^3)$$

$$+ \mu I_1 \left(1 + \left(1 - \frac{1}{m}\right)p + \mathcal{O}(p^2)\right) \tag{4.25}$$

for method (4.1) and

$$Y_1 = 1 + p + \frac{1}{2}\left(1 - \frac{1}{m}\right)p^2 + \mathcal{O}(p^3) + \mu I_1\left(1 + \left(1 - \frac{1}{m}\right)p + \mathcal{O}(p^2)\right)$$
$$+ \mu^2 I_{11}\left(1 + \left(1 - \frac{1}{m}\right)p + \mathcal{O}(p^2)\right) \tag{4.26}$$

for method (4.12). We now compute the leading error terms for the local weak and strong truncation errors. For the weak error, we take $G(y) = y$. For the local strong error, we will use $(\mathbb{E}(|Y(h) - Y_1|^2))^{1/2}$ as a measure of the error, since this expression is easier to handle for the computations which follows.[1] Comparing (4.24) with (4.25) we get for methods (4.1)

$$|\mathbb{E}(Y(h)) - \mathbb{E}(Y_1)| = \frac{(h\lambda)^2}{2m} + \mathcal{O}(h^3) \tag{4.27}$$

$$\left(\mathbb{E}(|Y(h) - Y_1|^2)\right)^{1/2} = \frac{h\mu^2}{2} + \mathcal{O}(h^{3/2}) \tag{4.28}$$

and comparing (4.24) with (4.26) we get for methods (4.12)

$$|\mathbb{E}(Y(h)) - \mathbb{E}(Y_1)| = \frac{(h\lambda)^2}{2m} + \mathcal{O}(h^3) \tag{4.29}$$

$$\left(\mathbb{E}(|Y(h) - Y_1|^2)\right)^{\frac{1}{2}} = h^{\frac{3}{2}}\left(\left(\frac{\lambda\mu}{m}\right)^2 + \mu^6\right)^{\frac{1}{2}} + \mathcal{O}(h^2). \tag{4.30}$$

We observe that changing the stage number of the S-ROCK methods does decrease the error constant in the weak local error, for both methods (4.1) and (4.12). For the strong local error, the error constant decreases for method (4.12) and is bounded independently of the stage number for method (4.1). These observations are important, since they indicate that the error growth is stable with respect to stage order changes. Numerical experiments in section 5 confirm these findings.

5. Numerical examples and applications

We first test numerically the convergence results obtained for the S-ROCK methods. We then present a simulation of a chemical reaction, involving multi-dimensional stiff Itô-SDEs.

5.1. Numerical study of S-ROCK methods.
To study the convergence properties of the S-ROCK methods, we consider the linear test problem (2.6) for which we have a known solution (see section 2.2). We numerically solve the test problem with the S-ROCK methods (4.1) (strong order 1/2) and (4.12) (strong order 1) for various stage numbers ($m = 3, 10, 200$).

Strong error. We choose $\lambda = 2, \mu = 1$. To estimate the error in the strong sense at time $T = 1$ for various stepsizes h. We choose N such that $Nh = 1$ and approximate

$$e_h^{\text{strong}} := \mathbb{E}|Y_N - Y(T)| \tag{5.1}$$

by averaging the endpoint error over $N = 5 \cdot 10^4$ numerically generated paths. The sampling error, which is known to decay as $1/\sqrt{N}$, is negligible here. We see in

---

[1] We notice that a strong local error of order ρ in this norm implies a strong local error of order ρ for (2.3) because of the Chebyshev inequality.

figures 5.1 and 5.2 that we obtain the expected rate of convergence. Furthermore, the precision is independent of the stage number for the methods (4.1) and increases as we increase the number of stages for the methods (4.12). This is due to the decrease of the error constants as studied in section 4.3 (see estimates (4.28) and (4.30)).

Weak error. The next test is with respect to weak convergence. We choose $G(y) = y$ in (2.5) and estimate the weak error at time $T = 1$ for various stepsizes h. We choose N such that $Nh = 1$ and approximate

$$e_h^{\text{weak}} := |\mathbb{E}(Y_N) - \mathbb{E}(Y(T))|, \tag{5.2}$$

where $\mathbb{E}(Y(T)) = Y_0 \exp(\lambda T)$ for the problem (2.6). We average over $N = 5 \cdot 10^4$ samples. Here we choose the parameters $\lambda = 2, \mu = 0.1$. We see in figures 5.1 and 5.2 that we obtain the expected convergence. We also see that, as we increase the number of stages, we obtain better accuracy. This is due to the behavior of the error constants studied in section 4.3 (see estimates (4.27) and (4.29)).
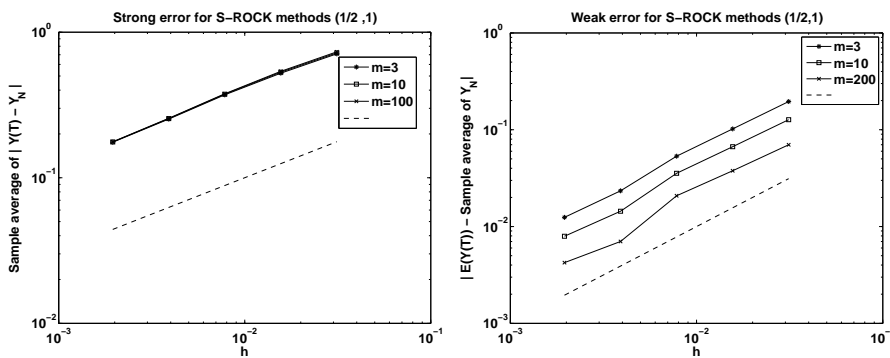

FIG. 5.1. *Strong and weak error plots for the strong order $1/2$ S-ROCK methods with various stage numbers. The dashed line is the reference straight line with slope $1/2$ (left plot) and slope 1 (right plot).*
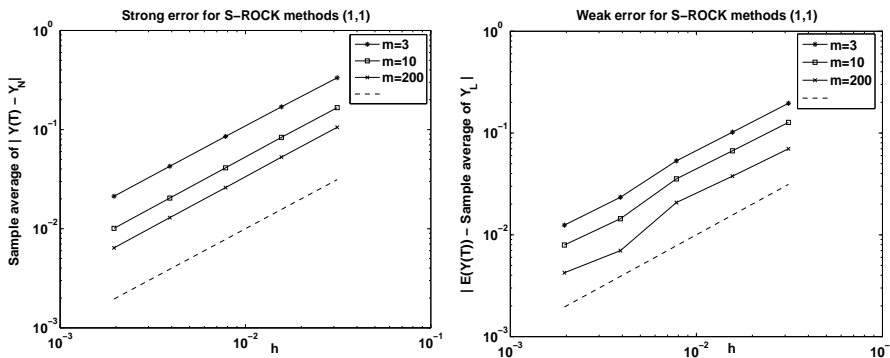

FIG. 5.2. *Strong and weak error plots for the strong order 1 S-ROCK methods with various stage numbers. The dashed line is the reference straight line with slope 1 (left and right plots).*

REMARK 5.1. In this paper, we have restricted ourselves to S-ROCK methods with $m \leq 200$. A higher stage number would improve the efficiency discussed above for stiff problems. However, some care should be taken since accumulation of round-off error and so-called internal stability issues can arise in the $m-1$ deterministic steps for $m \gg 200$ [24].

5.2. A nonlinear stiff problem. To highlight the necessity to include a whole "portion" of the stability domain of the linear test problem in the stability domain of a numerical method (see (2.13)), we consider the following nonlinear problem

$$dY = -\lambda Y(1-Y)dt - \mu Y(1-Y)dW_t, \quad Y(0) = Y_0, \qquad (5.3)$$

which is a normalized version of a population dynamics model (see [8, Chap. 6.2]). A linearization about the stationary solution $Y(t) \equiv 1$ leads to the linear test problem (2.6) considered in the previous example. We plot in Figure 5.3 a typical trajectory (computed with the Euler-Maruyama method) over the time interval $[0,1]$ with starting value $Y_0 = 0.9$ and parameters $\lambda = -4, \mu = -\sqrt{-2(\lambda+1)}$. In what follows, we will increase the value of $|\lambda|$ which in turn will increase the stiffness of the problem. We note that the chosen pair (λ, μ) is close to the boundary of the stability region of the linear test problem. At the same time, this choice ensures that $\lambda + \mu^2/2 = -1 < 0$ which is required by (2.7). We next take a collection of parameters
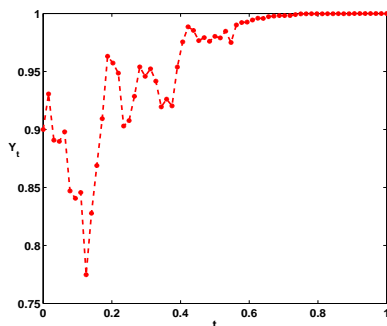

FIG. 5.3. *Sample of the process given by (5.3) computed with the Euler-Maruyama method* $(Y_0 = 0.9, \lambda = -4, \mu = -\sqrt{-2(\lambda+1)})$.

$(\lambda, -\sqrt{-2(\lambda+1)})$ and, as mentioned above, increase the stiffness by selecting successively $\lambda = -10, -10^2, -10^3, -10^4$. We numerically solve the problem (5.3) for these sets of parameters with the Euler-Maruyama and the S-ROCK methods. To study the mean square stability, we choose a starting value $Y_0 = 0.9$ at $t = 0$, close to the stationary solution $Y(t) \equiv 1$ and estimate the deviation to this solution at time $T = 1$. As a measure of the error, we compute the strong error (5.1) by averaging the endpoint error over $N = 10^5$ numerically generated paths. The sampling error, which is known to decay as $1/\sqrt{N}$ is negligible here. In all the experiments, we ask that $e_h^{\text{strong}} \leq tol$ and we choose the stepsize as $h = 2^{-n}$ (the precise value of tol is not important as we want only to check stability; the value of $tol = 10^{-3}$ was chosen in the experiments). For the Euler-Maruyama method, this requirement can only be achieved upon reducing the stepsize in view of its small stability domain. For the S-ROCK method, we fix the stepsize for all the values of λ and μ and vary the stage number to achieve a stable

integration. The choice of $h = 2^{-3}$ ensures $e_h^{\text{strong}} \leq tol$ for all the experiments. We collect the results in Table 5.1. As a measure of the numerical work, we monitor the function evaluations. The quantity $\sharp f$ represents the number of drift evaluations (for one sample path) while $\sharp g$ represents the number of diffusion evaluations (again for one sample path). Note that for both methods, we have for each diffusion evaluation also to generate a random number, thus $\sharp g$ counts as well the number of generated normal random variables.

TABLE 5.1. *Work versus stiffness for Euler-Maruyama (EM) and the S-ROCK methods*

	$\lambda = -10$	$\lambda = -10^2$
EM	$\sharp f = 128,\ \sharp g = 128$	$\sharp f = 4096,\ \sharp g = 4096$
stepsize	$h = 2^{-7}$	$h = 2^{-12}$
S-ROCK	$\sharp f = 24,\ \sharp g = 8$	$\sharp f = 40,\ \sharp g = 8$
stepsize (stage nb.)	$h = 2^{-3}\ (m = 3)$	$h = 2^{-3}\ (m = 5)$
	$\lambda = -10^3$	$\lambda = -10^4$
EM	$\sharp f = 16384,\ \sharp g = 16384$	$\sharp f = 262144,\ \sharp g = 262144$
stepsize	$h = 2^{-14}$	$h = 2^{-18}$
S-ROCK	$\sharp f = 160,\ \sharp g = 8$	$\sharp f = 520,\ \sharp g = 8$
stepsize (stage nb.)	$h = 2^{-3}\ (m = 20)$	$h = 2^{-3}\ (m = 65)$

We see in Table 5.1 the tremendous improvement of the efficiency when switching from the Euler-Maruyama to the S-ROCK methods. Note that for the actual cost of the experiments, these results have to be multiplied by the number of samples (here 10^5) which leads to a significant difference in computing time for the two methods. Note also that the time-step restriction in this example arising for the Euler-Maruyama method is much more severe than the restriction corresponding to the noise-free behavior. In the latter situation, we would have a maximum stepsize of $h = 2 \cdot 10^{-1}, 2 \cdot 10^{-2}, 2 \cdot 10^{-3}, 2 \cdot 10^{-4}$ for $\lambda = -10, -10^2, -10^3, -10^4$, several orders of magnitude larger than for the above experiments. This illustrates the necessity of including a whole "portion" of the stability domain of the linear test problem and the necessity of the damping strategy in the S-ROCK method as discussed in section 4.

5.3. A "non mean-square stable" fast slow system. The following example illustrates that some care should be taken when adding noise to a deterministic stiff system. This example also shows that the stability concept considered in this paper, namely the mean-square stability, does not cover some classes of interesting multiscale stochastic systems. Consider the singular perturbed problem

$$dx = f(x, y)dt,\ x(t_0) = x_0, \tag{5.4}$$

$$dy = \frac{1}{\varepsilon} g(x, y)dt,\ y(t_0) = y_0, \tag{5.5}$$

where $\varepsilon > 0$ is a small parameter. This equation represents a fast-slow system (y being the fast variable and x the slow one). Assuming a suitable dissipative condition for the fast system, it is well-known that the dynamics for the fast system (with the slow variable frozen) has a (Dirac) invariant measure and converges exponentially fast to a fixed point (invariant manifold) [10, Chap. 6]. The slow variable is well-approximated by a reduced problem with an effective force $\bar{f}$ (usually not available in explicit form) obtained by averaging f with respect to the invariant measure of

the fast system. From a numerical point of view, a standard numerical solver will have a stepsize restriction governed by stability issues in solving the fast system. This is a typical stiff system and stiff solvers such as implicit solvers or Chebyshev (e.g. ROCK) methods can overcome the aforementioned stepsize restriction [1, 2, 10]. In this situation, a stable integration leads also to an accurate solution.

If one includes a fast random perturbation in the above system, stable integration does no longer guarantee an accurate solution if the fast dynamics is not mean-square stable and has a non-trivial invariant dynamics. This issue has been discussed in [16] for implicit solvers and we illustrate it briefly for the S-ROCK methods. We add a suitably scaled additive white noise to the fast variable of the system (5.4) and consider

$$dx = f(x,y)dt, \ x(t_0) = x_0, \tag{5.6}$$

$$dy = \frac{1}{\varepsilon}g(x,y)dt + \sqrt{\frac{2}{\varepsilon}}dW(t), \ y(t_0) = y_0. \tag{5.7}$$

In what follows, we choose $f(x,y) = -y^2 + 5\sin(2\pi t)$ and $g(x,y) = x - y$. The fast
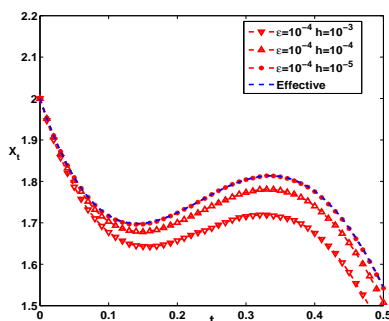

FIG. 5.4. *Solution for the slow variable of the system (5.6) integrated with the S-ROCK methods.*

system with the slow variable fixed is an Ornstein-Uhlenbeck process and the invariant distribution (for $t \to \infty$) is a stationary Gaussian process with mean x and variance 1. The effective forces can easily be computed (see [16] for details) and read $\bar{f}(x) = \int_{\mathbb{R}} f(x,y)\mu_x(dy) = -x^2 + 5\sin(2\pi t) - 1$. To illustrate the numerical behavior of the S-ROCK methods applied to this problem, we fix $\varepsilon = 10^{-4}$ and integrate the system (5.6-5.7) over the time interval $[0,0.5]$ with $x(0) = 2$ and $y(0) = 1$. We choose various time steps $h = 10^{-3}, 10^{-4}, 10^{-5}$. In each case, we adjust the number of stages to achieve a stable integration. Of course, an integration with a standard explicit solver would not be possible for time steps $h \geq \varepsilon$.

We see in Figure 5.4 that the integration is stable for all stepsizes, but accurate (i.e. close to the effective solution) only when $h < \varepsilon$, i.e., when the fast variable is resolved. An explanation of this behavior can be obtained following the procedure described in [16] for implicit solvers by computing an invariant numerical solution for the S-ROCK methods applied to the fast system (5.7) with the slow variable fixed. Note that this invariant solution involves the stability functions (4.9) of the S-ROCK methods. A similar behavior was observed for implicit methods in [16], but while there is not enough dissipation for the numerical invariant measure of the S-ROCK

methods, there is too much dissipation for implicit solvers. We close this discussion by recalling that the above problem is *not mean-square stable* and the behavior of the S-ROCK method is thus not in contradiction with the favorable properties of these methods (as constructed in this paper) for stiff mean-square stable problems. Drawing an analogy to ODEs, systems such as (5.6-5.7) exhibit a behavior closer to oscillatory problems which are not considered as stiff and which are usually poorly integrated with classical stiff solvers. The multiscale methods developed in [25] and [7] which rely on averaging theorems instead of stability concepts can handle such fast-slow systems as considered in this example. These methods compute the average forces of the slow system on the fly, relying on a resolved computation of the fast system over a short period of time.

5.4. Application: simulation of stiff chemical systems. We illustrate the use of the Itô S-ROCK methods on an important application: the simulation of a stiff system of chemical reactions given by the Chemical Langevin Equation (CLE). We consider a system of reactions, the so-called Michaelis-Menten system, describing the kinetics of many enzymes. The reactions involve four species: S_1 (a substrate), S_2 (an enzyme), S_3 (an enzyme substrate complex), and S_4 (a product). The reactions can be described as follows: the enzyme binds to the substrate to form an enzyme-substrate complex which is then transformed into the product, i.e.,

$$S_1 + S_2 \xrightarrow{c_1} S_3 \tag{5.8}$$

$$S_3 \xrightarrow{c_2} S_1 + S_2 \tag{5.9}$$

$$S_3 \xrightarrow{c_3} S_2 + S_4. \tag{5.10}$$
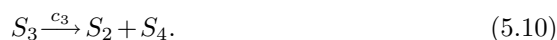
The mathematical description of this kinetic process can be found in [13]. The state-change vectors corresponding to these reactions are $\nu_1 = (-1, -1, 1, 0)^T$, $\nu_2 = (1, 1, -1, 0)^T$, $\nu_3 = (0, 1, -1, 1)^T$. For the simulation of this set of reactions we use the CLE model

$$dY(t) = \sum_{j=1}^{3} \nu_j a_j(Y(t)) dt + \sum_{j=1}^{3} \nu_j \sqrt{a_j(Y(t))} dW_j(t), \tag{5.11}$$

where $a_j(Y(t))$ are the so-called propensity functions given by

$$a_1(Y(t)) = c_1 Y_1 Y_2, \ a_2(Y(t)) = c_2 Y_3, \ a_3(Y(t)) = c_3 Y_3.$$

We set the initial amount of species as

$$Y_1(0) = [5 \times 10^{-7} n_A vol], Y_2(0) = [5 \times 10^{-7} n_A vol], Y_3(0) = 0, Y_4(0) = 0,$$

where $[\cdot]$ denotes the rounding to the next integer and $n_A = 6.023 \times 10^{23}$ is Avagadro's constant (number of molecules per mole) and *vol* is the volume of the system. The parameters of the system are borrowed from [26, Section 7.3]. A computational study of this problem with various simulation techniques (from Monte-Carlo methods, SDE and ODE solvers) is reported in [11]. In the following numerical experiments, the focus is on the behavior of the S-ROCK methods when the parameters of the problem lead to increasingly stiff systems. We compare the S-ROCK methods with the Euler-Maruyama method, widely used for such problems. While the S-ROCK methods are as simple to use and implement as the Euler-Maruyama method, we see below that

the former methods are significantly more efficient as the stiffness of the problem increases.

We integrate the CLE on the time interval $[0,50]$. For this problem with multidimensional Wiener processes, we use the S-ROCK methods (4.1). We see in Figure 5.5 that for a set of reaction rates leading to a nonstiff system we have the same behavior for the Euler-Maruyama and the S-ROCK methods. We next increase the rate of the
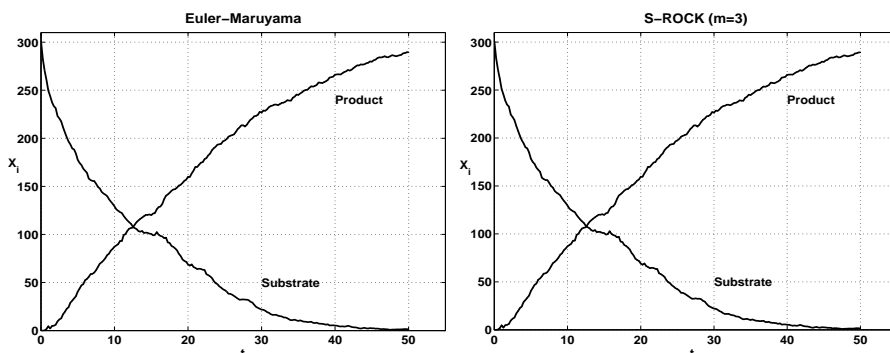

FIG. 5.5. *Shown above is one trajectory of the Michaelis-Menten system solved with the Euler-Maruyama method (left plot) and the S-ROCK method (right plot) for $c_1 = 1.66 \times 10^{-3}, c_2 = 10^{-4}, c_3 = 0.10$. The stepsize is $h = 0.25$ for both methods, $m = 3$ for S-ROCK. The same Brownian path is used for both methods.*

third reaction in (5.8)–(5.10), $c_3 = 10^2, 10^3, 10^4$ corresponding to an increasingly fast production. The resulting CLE become stiff and the Euler-Maruyama method is inefficient. In Figure 5.6 we report the stepsize and the number of function evaluations needed for the Euler-Maruyama and the S-ROCK methods. By number of function evaluations we mean here the total number of drift and diffusion evaluations. Writing (5.11) as $dY = f(Y)dt + g(Y)dW(t)$ where f and W are vectors and g is a matrix, each evaluation of $f(Y)$ or $g(Y)dW(t)$ are counted as one function evaluation. For both methods, one evaluation of $g(Y)dW(t)$ is needed per time-step. Thus, by keeping a fixed time step, the number of generated random variables remains constant as the stiffness increases for the S-ROCK methods, while this number increases with the stepsize reduction of the Euler-Maruyama method.

The Euler-Maruyama method faces step-size reduction as can be seen in Figure 5.6. Starting from $h = 0.25$ the stepsize is progressively decreased to 1.85×10^{-4} in order to have a stable integration and the number of function evaluations grows accordingly.

For the S-ROCK method, we can fix $h = 0.25$ for all the simulations and vary the number of stages (from $m = 3$ to $m = 81$) in order to handle the stiffness. Taking advantage of the quadratic growth of the stability domains, we see that the number of function evaluations needed is reduced by several orders of magnitude compared to the Euler-Maruyama method.

Finally we should remark that negative populations may appear during the computation. In this case, the computation of the diffusion term is not possible. To circumvent this issue, we take absolute value in the square root as usually done in the literature (see for example [11]). Though in the continuous case, negative populations do not appear, it is a common problem in the numerical discretization of chemical reaction processes, even for the reaction rate equation (RRE) without noise [10]. For
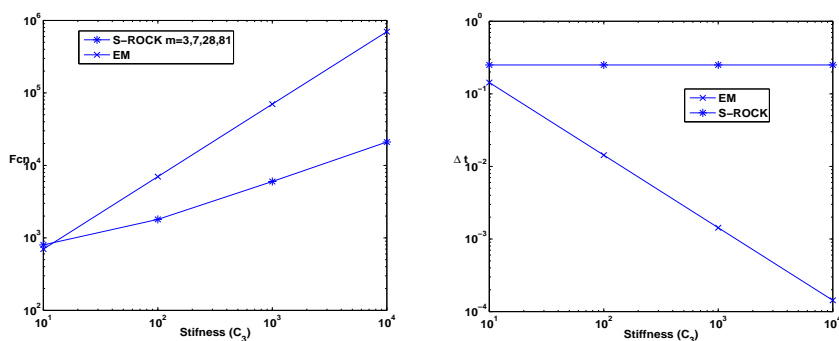
FIG. 5.6. *The Michaelis-Menten system solved with the Euler-Maruyama and the S-ROCK methods with increasing rate constant c_3. The stepsize is chosen as $h = 0.25$ for the S-ROCK methods. For the Euler-Maruyama we select for each value of c_3 the maximum stepsize which leads to a stable integration. For the Euler-Maruyama method, stability is achieved by reducing the step-size, for the S-ROCK method by increasing the stage number ($m = 3, 7, 28, 81$).*

our chemical reaction problem, we may argue that we actually solve a modified equation with an absolute value for $a_j(Y)$ in the diffusion term. But more systematic strategy for solving this type of problem avoiding negative populations need to be explored. This is the subject of an ongoing research project.

REFERENCES

[1] A. Abdulle and A.A. Medovikov, *Second order Chebyshev methods based on orthogonal polynomials*, Numer. Math., 90, 1–18, 2001.

[2] A. Abdulle, *Fourth order Chebyshev methods with recurrence relation*, SIAM J. Sci. Comput., 23, 2041–2054, 2002.

[3] A. Abdulle and S. Cirilli, *Stabilized methods for stiff stochastic systems*, C. R. Acad. Sci. Paris, 345, 593–598, 2007.

[4] A. Abdulle and S. Cirilli, *S-ROCK methods for stiff stochastic problems*, SIAM J. Sci. Comput., 30, 997–1014, 2008.

[5] L. Arnold, *Stochastic Differential Equations, Theory and Application,* Wiley, 1974.

[6] K. Burrage and P.M. Burrage, *Order conditions of stochastic Runge-Kutta methods by B-series,* SIAM J. Numer. Anal., 38, 1626–1646, 2000.

[7] W. E, D. Liu, and E. Vanden-Eijnden, *Analysis of multiscale methods for stochastic differential equations*, Comm. Pure Appl. Math., 1–48, 2004.

[8] T.C. Guard, *Introduction to Stochastic Differential Equations*, Marcel Dekker, New York, 1988.

[9] A. Guillou and B. Lago, *Domaine de stabilité associé aux formules d'intégration numérique d'équations différentielles, à pas séparés et à pas liés. Recherche de formules à grand rayon de stabilité*, 1er Congr. Assoc. Fran. Calcul (AFCAL), Grenoble, 43–56, 1960.

[10] E. Hairer and G. Wanner, *Solving Ordinary Differential Equations II. Stiff and Differential-Algebraic Problems*, Second edition, Springer-Verlag, Berlin and New York, 1992.

[11] D.J. Higham, *Modelling and Simulating Chemical Reactions*, SIAM Review, to appear, 2008.

[12] P.J. van der Houwen and B.P. Sommeijer, *On the internal stage Runge-Kutta methods for large m-values*, Z. Angew. Math. Mech., 60, 479–485, 1980.

[13] N.G. van Kampen, *Stochastic Processes in Physics and Chemistry*, Elsevier Sciences, Netherlands, 1992.

[14] P.E. Kloeden and E. Platen, *Numerical Solution of Stochastic Differential Equations*, Springer-Verlag, Berlin and New York, 1992.

[15] V.I. Lebedev, *How to solve stiff systems of differential equations by explicit methods*, CRC Pres, Boca Raton, 45–80, 1984.

[16] T. Li, A. Abdulle and Weinan E, *Effectiveness of implicit methods for stiff stochastic differential equations*, Commun. Comput. Phys., 3, 295–307, 2008.

[17] G. Maruyama, *Continuous Markov processes and stochastic equations*, Rend. Circolo Math. Palermo, 4, 48–90, 1955.

[18] G.N. Milstein, *Approximate integration of stochastic differential equations*, Theor. Prob. Appl., 19, 557–562, 1974.

[19] G.N. Milstein and M.V. Tretyakov, *Stochastic Numerics for Mathematical Physics*, Scientific Computing, Springer-Verlag, Berlin and New York, 2004.

[20] B. Oksendal, *Stochastic Differential Equations*, Sixth Edition, Springer-Verlag, Berlin and New York, 2005.

[21] E. Platen, *Zur Zeitdiskreten Approximation von Itôprozessen*, Diss. B. Imath. Akad. des Wiss. der DDR, Berlin, 1984.

[22] A. Rössler, *Runge-Kutta Methods for the Numerical Solution of Stochastic Differential Equations*, Shaker Verlag, Aachen, 2003.

[23] Y. Saitô and T. Mitsui, *Stability analysis of numerical schemes for stochastic differential equations*, SIAM J. Numer. Anal., 33, 2254–2267, 1996.

[24] B.P. Sommeijer, L.F. Shampine and J.G. Verwer, *RKC: an explicit solver for parabolic PDEs,* J. Comput. Appl. Math., 88, 316–326, 1998.

[25] E. Vanden-Eijnden, *Numerical techniques for multiscale dynamical system with stochastic effects*, Commun. Math. Sci., 1, 385–391, 2003.

[26] D.J. Wilkinson, *Stochastic Modelling for Systems Biology*, Chapman and Hall/CRC, 2006.